J. Fluid Mech. (1978), *vol.* 85, *part* 4, *pp.* 705–730
Printed in Great Britain

The growth of duration-limited wind waves

By HISASHI MITSUYASU
AND KUNIO RIKIISHI

Research Institute for Applied Mechanics,
Kyushu University, Fukuoka, Japan

(Received 14 October 1975 and in revised form 4 August 1977)

Laboratory measurements have been made of the one-dimensional spectra of the duration-limited wind waves which are generated when a wind abruptly begins to blow over a water surface, maintaining a constant speed during the succeeding period of time. The duration dependences of the wave energy E and the spectral peak frequency f_m determined from the measured spectra are slightly different from those inferred from the fetch dependences of these quantities. The normalized spectra of the duration-limited wind waves are also slightly different from those of fetch-limited wind waves: the concentration of the normalized spectral energy near the spectral peak frequency is smaller, in many cases, for the duration-limited wind waves than for fetch-limited wind waves. The exponential growth rates β of the duration-limited wind-wave spectra are generally larger than those of fetch-limited wind-wave spectra. Furthermore, both for the duration-limited wind waves and for fetch-limited wind waves the exponential growth rate has a behaviour which is different from the empirical formula of Snyder & Cox (1966). A new empirical formula for the growth rate of the wave spectrum is proposed, from which the empirical formula of Snyder & Cox (1966) can be derived as a special case. Agreement between the new empirical formula and the experimental results is satisfactory for fetch-limited wave spectra, but is confined to the qualitative features for the duration-limited wave spectra.

1. Introduction

Many observations of the spectra of fetch-limited wind waves have been made both in the ocean and in laboratory tanks to clarify the growth mechanisms of wind-generated waves. However, with regard to the growth of duration-limited wind waves, laboratory experiments are quite few apart from the preliminary study by Hidy & Plate (1966) and the recent study by Larson & Wright (1975), though several field observations have been made (Inoue 1966; Iwata & Tanaka 1970; DeLeonibus & Simpson 1972; Taira 1972). According to these field observations, the exponential growth rates β determined from duration-limited wind waves (Iwata & Tanaka 1970; DeLeonibus & Simpson 1972; Taira 1972) are almost the same as those determined from fetch-limited wind waves (Barnett 1968). However, our preliminary study in a laboratory tank (Mitsuyasu & Rikiishi 1972) has shown that the growth rate β of duration-limited wind waves is much larger than that of fetch-limited wind waves, though the values of β for fetch-limited wind waves are consistent with the empirical formula proposed by Barnett (1968). One of the purposes of the present study is to confirm the results of our preliminary study.

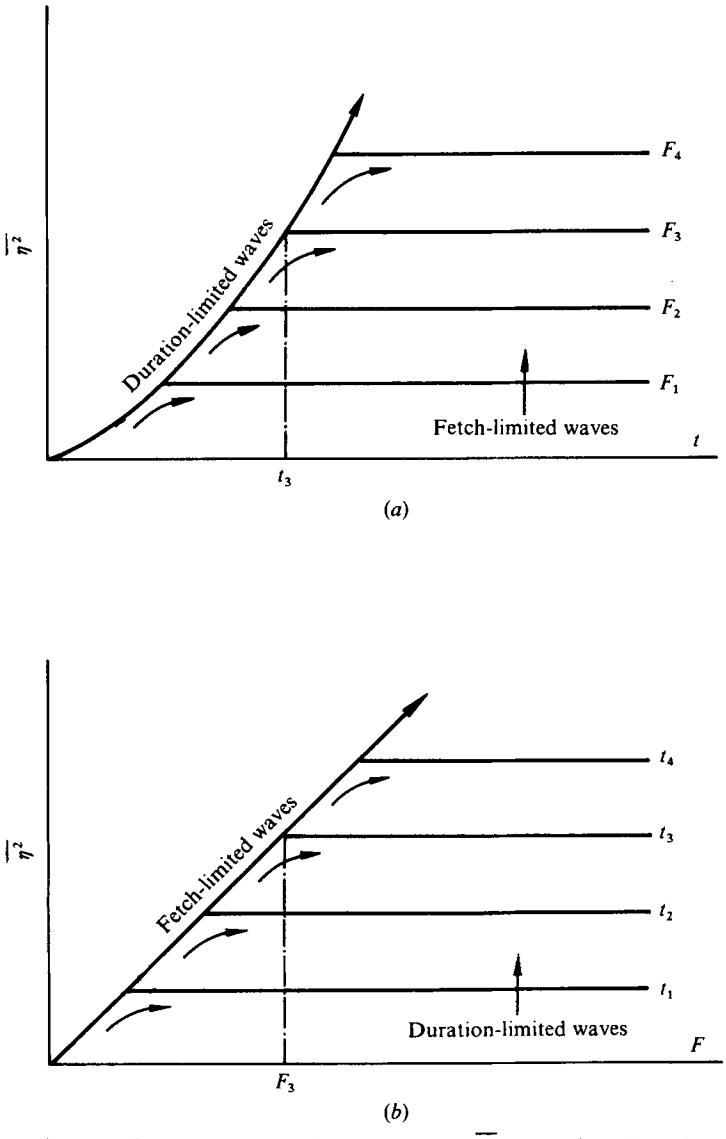

FIGURE 1. Schematic growth curves of wind-wave energy $\overline{\eta^2}$ for a duration time t or fetch F with a fixed wind speed. (*a*) $\overline{\eta^2}$, t curve for various fetches F. (*b*) $\overline{\eta^2}$, F curve for various duration times t.

Another purpose of the present study is to compare the spectral forms of duration-limited wind waves with those of fetch-limited wind waves. According to the many observations of the spectra of fetch-limited wind waves, the one-dimensional spectra exhibit a similarity form with a very small deviation (Colonel 1966; Hidy & Plate 1966; Liu 1971; Mitsuyasu 1973; Hasselmann *et al.* 1973). However, the similarity of the spectral form has not been studied for the case of duration-limited wind waves.

Therefore the present study is designed to obtain accurate data on the successive spectra of duration-limited wind waves generated in a laboratory tank under carefully

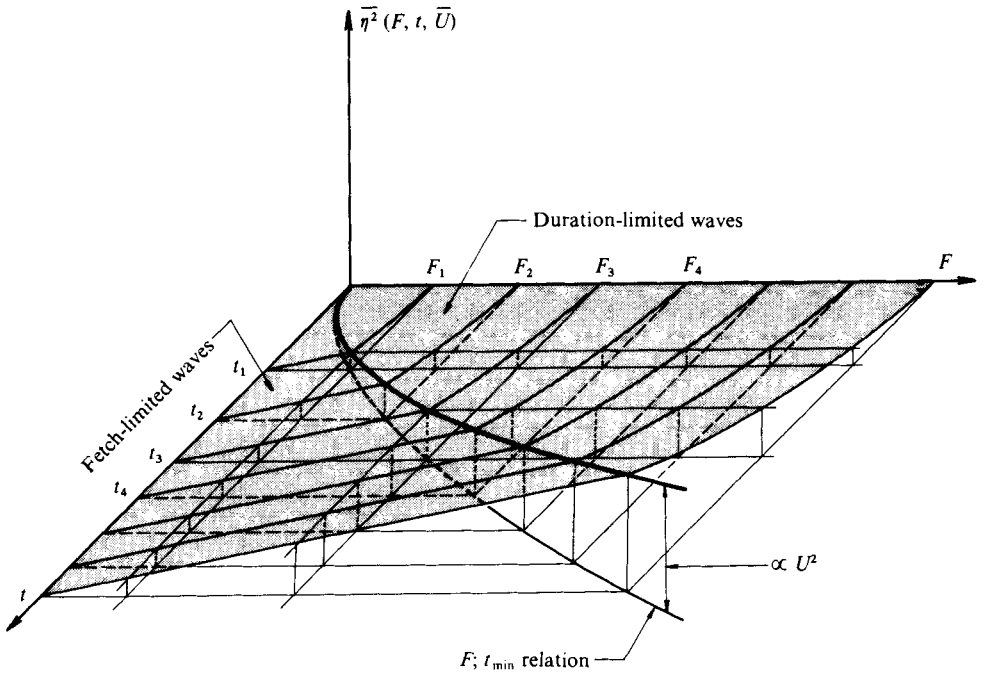

FIGURE 2. Schematic growth surface of wind-wave energy $\overline{\eta^2}$ for a duration time t, fetch F and a fixed wind speed U.

controlled conditions. The results are systematically compared with the accumulated data on fetch-limited wind waves in a steady state.

2. Fetch-limited wind waves and duration-limited wind waves

When a wind begins to blow over a still water surface of unlimited extent, maintaining a constant average speed and direction, tiny ripples are generated which develop with time uniformly over the entire water surface and finally develop into the huge waves observed in the ocean. In this case, the wave spectrum must be determined by only the duration and speed of the wind. Wind waves are duration limited (or unsteady) but spatially homogeneous. On the other hand, if the water area or the wind area has an upwind boundary, the wave spectrum saturates successively from the upwind end of the generating area and attains a steady state as shown schematically in figure 1, though the waves are developing with fetch even in that steady-state area. In this case of fetch-limited wind waves, the spectrum must be determined by only the fetch and the wind speed.

Even in the latter case, however, at any given instant t_3, say, wind waves are still duration limited in some leeward area $F > F_3$ very far from the upwind boundary if the duration t_3 is smaller than the minimum duration $t_{\min}$ for the fetch F in that area. Here the minimum duration $t_{\min}$ means the time necessary for the wave energy to travel from the upwind boundary to the position in which we are interested. Therefore, at any duration t_3, the wind-wave field can be divided into two regions: the fetch-limited region $F < F_3$, where the waves are steady and dependent only on F,

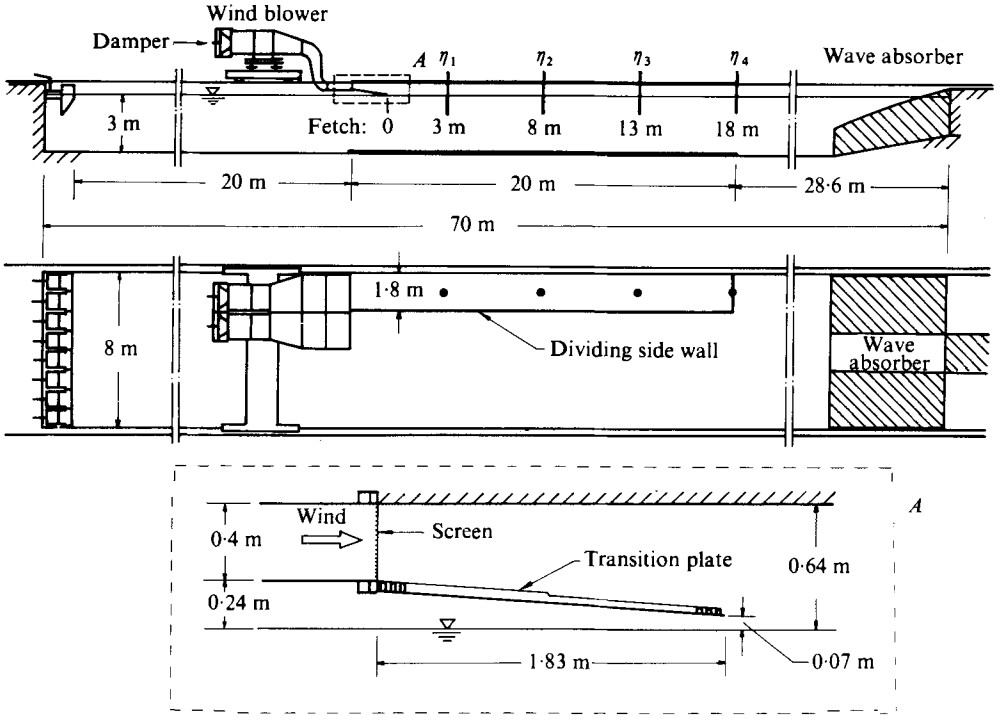

FIGURE 3. Wind-wave tank. The plunger is not used and only the divided part of the tank is used for the present experiment.

and the duration-limited region $F > F_3$, where the waves are unsteady but independent of F. The boundary F_3 between these two regions is considered as the front of the steady state, and is determined as the fetch for which the given duration t_3 is equal to the minimum duration t_{min}. The situations discussed above can be shown more generally as in figure 2, from which figure 1 can be derived as the projection of $\overline{\eta^2}(F, U)$ on (*a*) the $\overline{\eta^2}, t$ plane or on (*b*) the $\overline{\eta^2}, F$ plane. It can be seen from these figures that the wind waves in such simple conditions are either fetch limited or duration limited.

In a strict sense, however, the front of the steady state is not as sharp as in the schematic figures, and some transition region can be seen near the wave front. Therefore there exists a region where the wind waves are limited by both duration and fetch. Moreover, the wind speed and direction in the ocean change with time and space in many cases. This variability of the wind also causes waves which are both fetch and duration limited in the ocean.

In any event, the present study concerns mainly duration-limited wind waves in finite fetches which are generated when the duration time t is smaller than the minimum duration t_{min}.

3. Experimental equipment and procedure

The wind-wave tank

The experiment was conducted in a large wave tank at Tsuyazaki Laboratory, Kyushu University. Figure 3 shows the general layout of the wave tank. A closed test section which is similar to an ordinary wind-wave channel was constructed in the towing tank by adding a dividing side wall and a ceiling and by installing a wind blower. The width of the test section is 1·8 m, the height of air gap is 0·64 m, the water depth is 3 m and the length of the test section is 20 m from the outlet mouth of the wind blower. At the end of the test section wind waves spread out into the large section of width 8 m and are finally absorbed by the wave absorber at the end of the tank. Therefore wave reflexion in this tank is very small, less than 5 %. As shown in figure 3, a roughened transition plate was installed at the entrance of the test section to guide the air flow smoothly from the wind blower to the test section and to thicken the air boundary layer over the water surface.

Experimental procedure

By opening the damper of the wind blower very quickly from an open ratio $D = 0$ to $D = 15\,\%$, the wind speed was changed stepwise from zero to approximately 6·3 m/s,† maintaining this constant value during the succeeding period of time. A further series of experiments was made by changing the wind speed stepwise from zero to approximately 11 m/s and again holding it constant. However, the data from this series are used only for the analysis of steady-state fetch-limited wind waves and not for the analysis of duration-limited wind waves since the time required for the wind to reach a steady speed was about the same as the growth period of the waves.

Wind-generated waves were measured simultaneously at four stations (fetches $F' = 5$, 10, 15, 20 m) along the centre-line of the test section with resistance-type wave gauges and recorded continuously on a data recorder with seven channels. Because of the presence of the transition plate, the effective fetches F are 3, 8, 13 and 18 m.

The wind measurements

In order to monitor the variation of the wind speed during the measurements of wind waves, Pitot–static tubes were fixed at two stations $F = 3$ and 13 m (at a height of 20 cm above mean water surface), and connected to a dynamic strain meter through differential pressure transducers. Instantaneous values of the dynamic pressure $\frac{1}{2}\rho_a U^2$ were recorded on the data recorder simultaneously with the wave recording. The steady-speed wind profiles were measured at each wave observation station by traversing a Pitot–static tube. During the experiment the air temperature was slightly lower than the water temperature, but the differences did not exceed 1 °C.

† Cross-sectional mean speed at the test section.

D	F (m)	U_* (cm/s)	$\bar{U}_*$ (cm/s)	$Z_0 \times 10^3$ (cm/s)	$(gZ_0/U_*^2) \times 10^3$
15	3	31·1	31·1	6·75	6·83
	8	29·9	30·5	4·82	5·28
	13	29·9	30·3	4·96	5·44
	18	31·6	30·6	6·02	5·91
50	3	91·7	91·7	118	13·7
	8	88·3	90·0	91	11·4
	13	88·1	89·4	97	12·2
	18	89·6	89·4	112	13·7

TABLE 1. Wind data. D represents the open ratio (%) of the damper of the wind blower.

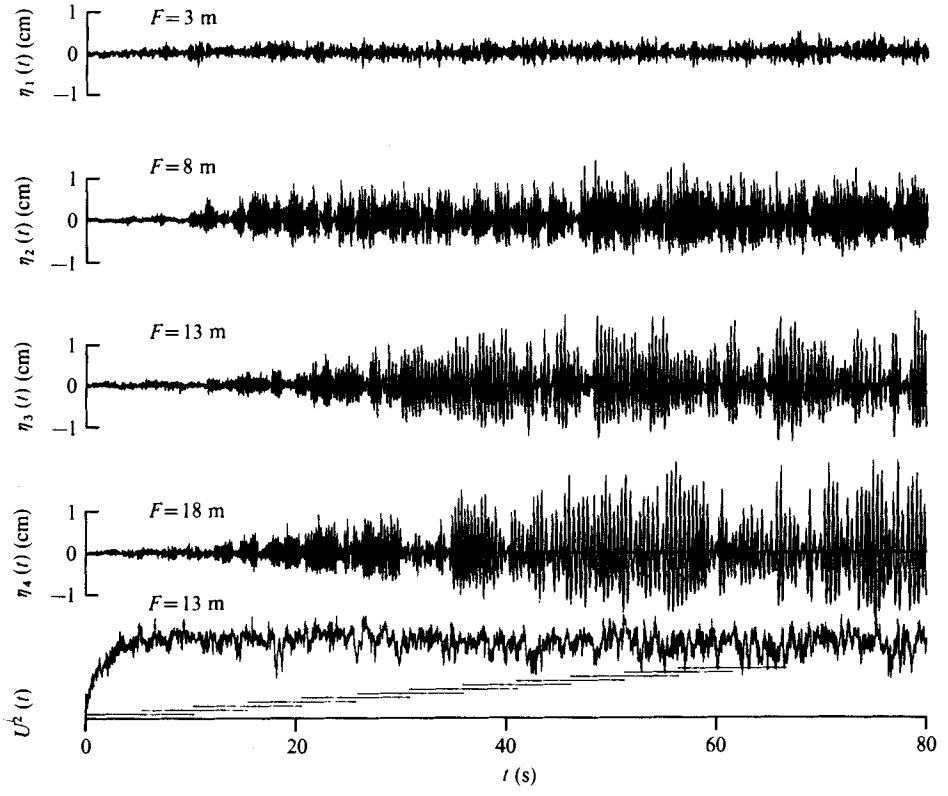

FIGURE 4. Initial part of the wind and wave records. The time axis is extremely compressed. $U^2(t)$ is shown on an arbitrary scale.

4. Experimental data and analysis

Wind profiles

Figure 4 shows the initial parts of the wind and wave records. The wind record at $F = 3$ m, not shown in this figure, was almost the same as that at $F = 13$ m, which is shown in the figure. As can be seen from this figure, the wind speed attains a constant value (steady state) in a short time, approximately 4 s.

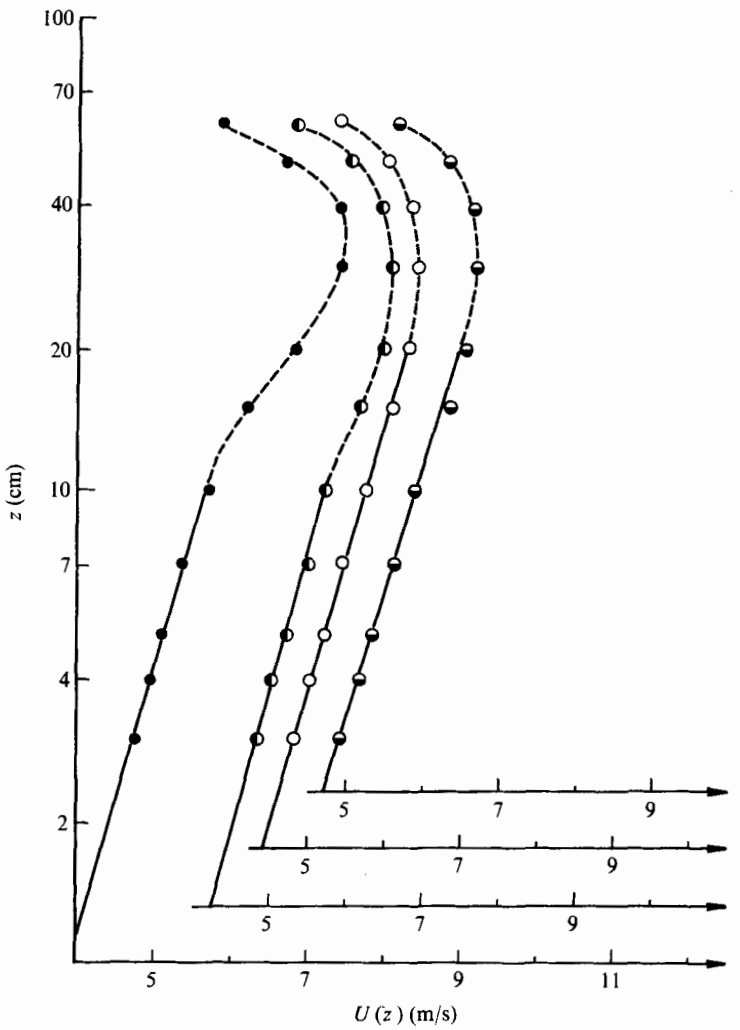

FIGURE 5. Wind profiles $U(z)$ over the water surface. Abscissa is shifted successively for different fetches. ●, $F = 3$ m; ◐, $F = 8$ m; ○, $F = 13$ m; ◒, $F = 18$ m.

In the steady state, measured wind profiles near the air–water interface follow a logarithmic distribution

$$U(z) = \frac{U_*}{\kappa} \ln \frac{z}{z_0}, \tag{1}$$

where $U(z)$ is the wind velocity at an elevation z above the mean water surface, U_* the friction velocity of the wind, κ the von Kármán constant and z_0 the roughness parameter. Figure 5 shows the wind profiles at each observation station. The friction velocity U_* and the roughness parameter z_0 were determined by fitting the logarithmic distribution (1) to the measured wind profiles. The measured values of U_*, z_0 and their dimensionless ratio gz_0/U_*^2 are shown in table 1. The present data on gz_0/U_*^2 are quite

similar to those measured by Hidy & Plate (1966). Since the local friction velocity U_* changes slightly with fetch, the mean friction velocity $\overline{U}_*^2$ within each fetch is introduced and is shown in table 1. The mean friction velocity $\overline{U}_*$ will be used hereafter as the reference wind velocity for the analysis of wind waves.

Spectral analysis of the wave data

The wave data recorded on magnetic tape were reproduced and digitized with a high-speed A/D converter. Spectral analysis of the data was performed on a FACOM 270-20 computer using a standard program based on fast-Fourier-transform procedures.

The wind waves in this study changed slowly with time and could not be considered statistically stationary. Although several complicated methods have been proposed for the spectral analysis of non-stationary random processes (see, for example, Priestley 1965, 1966, 1967), we adopt a simple method under the assumption of the quasi-stationarity of the phenomena. Wave data in the transient stage were divided into short segments of approximately 10 s so that the data could be considered approximately statistically stationary within each segment. Although the short length of the wave data widens the confidence band of the measured spectra, our recent study (Rikiishi & Mitsuyasu 1976) has shown that the dominant part of the spectrum is not seriously affected by the data length if the wave data contain more than approximately 20 waves. The various conditions for the data analysis were as follows: the length of a segment was 10·25 s and the sampling frequency 25 Hz with 256 data points in a segment. The spectral analysis of each segment of the wave data was done using a standard program based on fast-Fourier-transform procedures. Then a moving average of successive 15 line spectra was made by using a triangular filter. The number of degrees of freedom of the measured spectrum is approximately 20.

In practice, the segments of the wave data 10·25 s long were picked from the original data with overlaps of 5·125 s. Therefore we can obtain the wave spectra successively at 5·125 s intervals.

The locations of the segments in the unsteady parts of the wave data are shown in figure 4 and also in figure 6 as a group of short straight lines. Figure 6 shows the time variation of the wave energy $\overline{\eta^2}(t)$ at various fetches. Here $\overline{\eta^2}(t)$ was computed by taking a moving average of $\eta^2(t)$ with an averaging time of 5·125 s. The wave data in an interval 82 s long ($N = 2048$) in a steady region, the location of which is shown by a long straight line in figure 6, were used to obtain the spectra of the steady-state fetch-limited wind waves.

5. Growth of the wave spectrum with fetch and duration

Figure 7 shows the growth of the spectra of fetch-limited wind waves which were measured after the wind waves had already attained a steady state. The dependences of the wave energy E ($=\overline{\eta^2}$) and the spectral peak frequency f_m on fetch were determined from the measured wave spectra and are shown in figure 8, in dimensionless form. The fetch relations in figure 8 can be approximated by

$$gE^{\frac{1}{2}}/U_*^2 = 6{\cdot}70 \times 10^{-3}(gF/U_*^2)^{0{\cdot}641}, \tag{2}$$

$$U_* f_m/g = 1{\cdot}19(gF/U_*^2)^{-0{\cdot}357}, \tag{3}$$

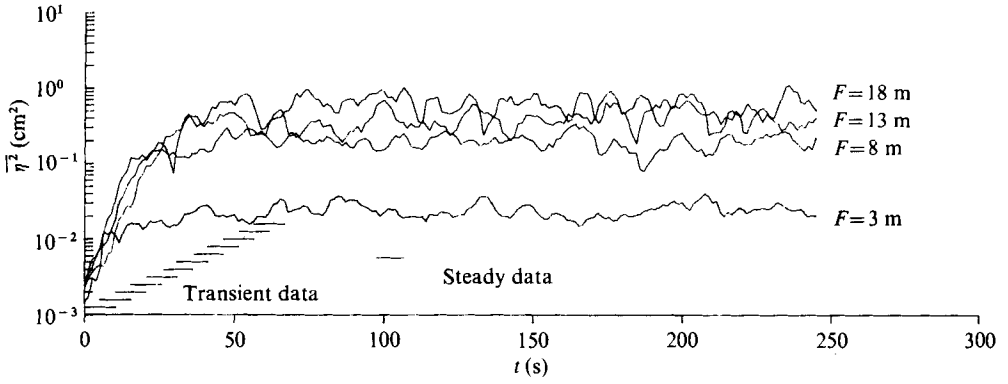

FIGURE 6. Time variation of the wave energy $\overline{\eta^2}$ at various fetches.

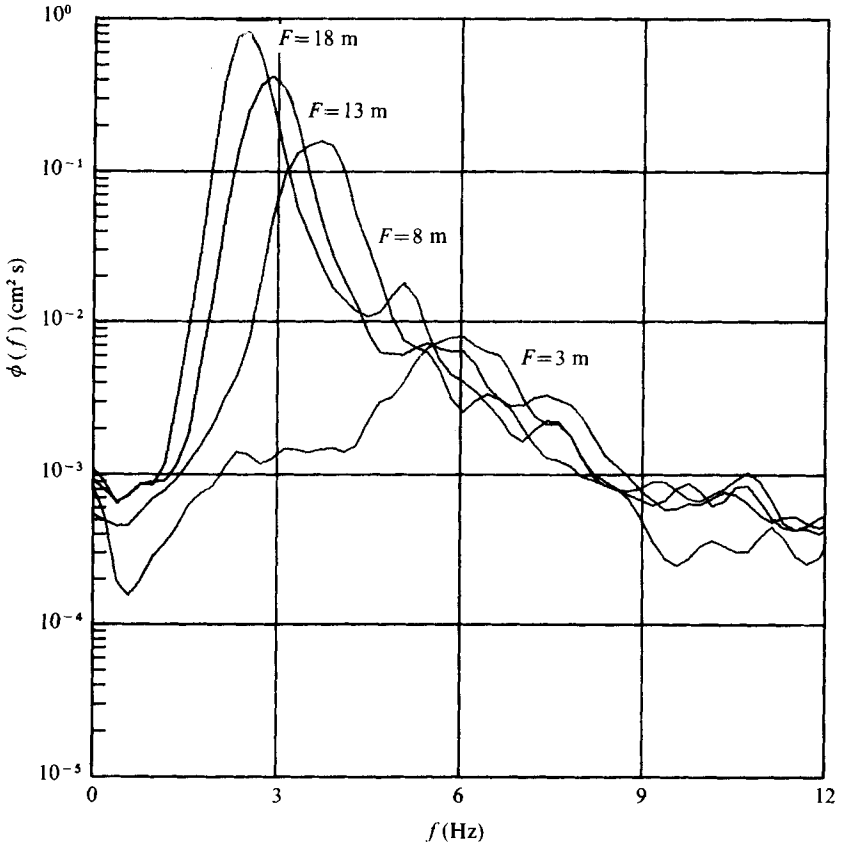

FIGURE 7. Growth of the wave spectrum with fetch.

where g is the acceleration due to gravity. In determining the fetch relations the wave data measured at F = 3 m were not used since those data show a trend which is slightly different from that of the data measured at longer fetches. A similar phenomenon was also found in a previous study (Mitsuyasu & Honda 1974).

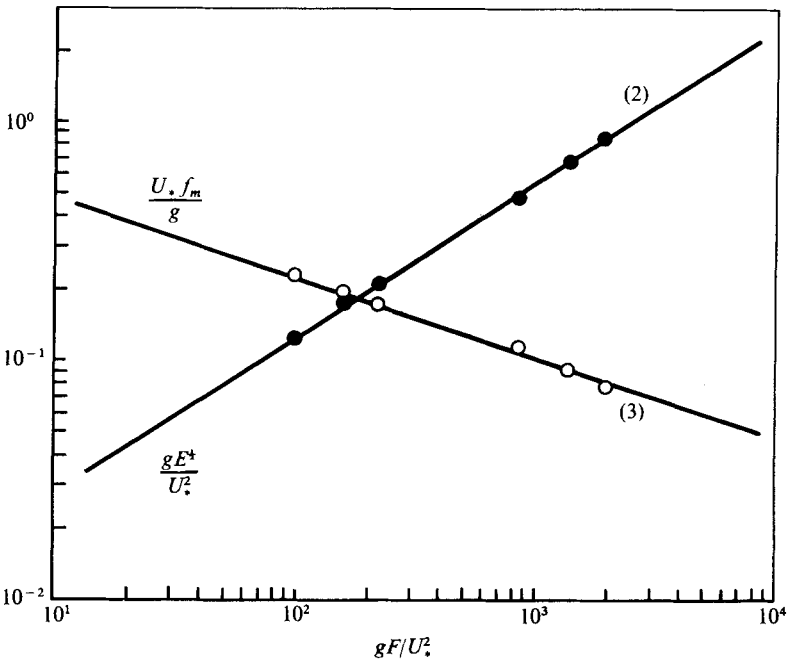

FIGURE 8. Fetch relations for the spectral peak frequency f_m and for the wave energy E. The data in the series of experiments with $\bar{U}_* = 89{\cdot}4$ cm/s were also used to determine the fetch relation.

The fetch relations (2) and (3) are slightly different from those determined in a previous study (Mitsuyasu 1968):

$$gE^{\frac{1}{2}}/U_*^2 = 1{\cdot}13 \times 10^{-2}(gF/U_*^2)^{0{\cdot}504}, \tag{4}$$

$$U_* f_m/g = 1{\cdot}00(gF/U_*^2)^{-0{\cdot}330}. \tag{5}$$

In the following discussion, however, (2) and (3) will be used.

Figures 9(*a*) and (*b*) show the growth of the spectra of the duration-limited wind waves at fetches $F = 13$ m and $F = 18$ m respectively. The numbers on each spectrum refer to the segment number, and the time interval between successive spectra is 5·125 s. The wave energy E and the spectral peak frequency f_m determined from these spectra are shown in dimensionless form in figure 10 as functions of duration time. Here the duration time t was measured from the time when the damper was opened. Owing to the transition time before the wind attains a constant speed, a small amount of uncertainty exists in the duration time. However, since the transition times are relatively short as stated previously, the errors due to the initial transition time are not serious for data corresponding to large duration times.

The solid straight lines

$$gE^{\frac{1}{2}}/U_*^2 = 1{\cdot}19 \times 10^{-4}(gt/U_*)^{1{\cdot}20}, \tag{6}$$

$$U_* f_m/g = 5{\cdot}16(gt/U_*)^{-0{\cdot}570} \tag{7}$$

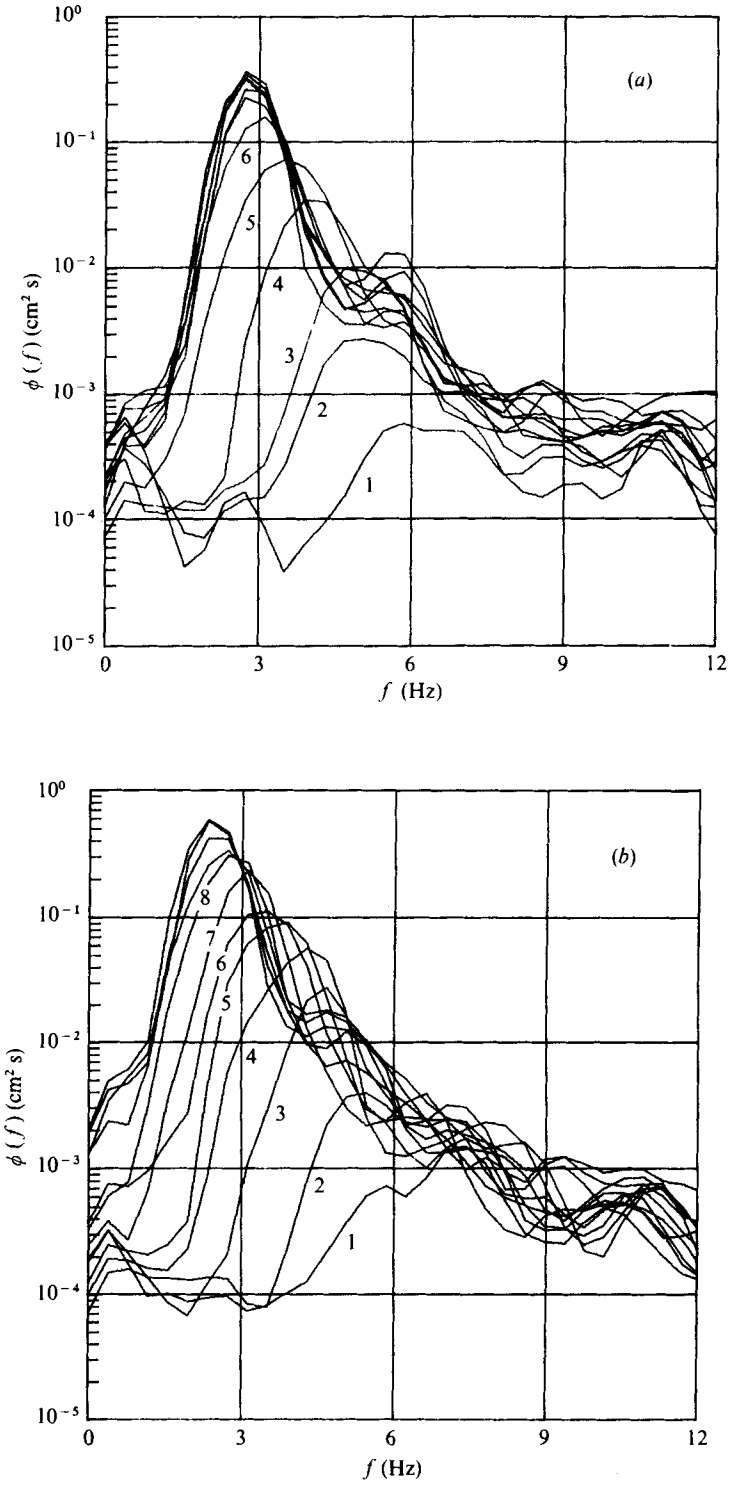

FIGURE 9. Growth of the wave spectrum with duration time. (*a*) $\bar{U}_* = 0$–30·3 cm/s, $F = 13$ m. (*b*) $\bar{U}_* = 0$–30·6 cm/s, $F = 18$ m.

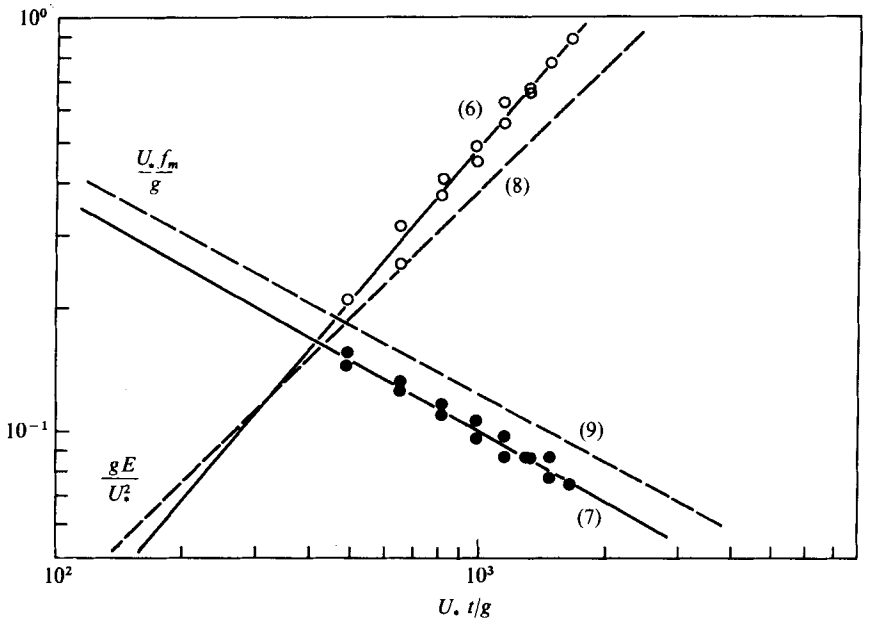

FIGURE 10. Duration relations for the spectral peak frequency f_m and for the spectral energy E. ——, best-fit relations (6) and (7); – – –, relations (8) and (9) inferred from the fetch relations.

in figure 10 represent the best-fit curves to the data. The broken straight lines

$$gE^{\frac{1}{2}}/U_*^2 = 3{\cdot}90 \times 10^{-4}(gt/U_*)^{0{\cdot}997}, \tag{8}$$

$$U_* f_m/g = 5{\cdot}80(gt/U_*)^{-0{\cdot}555} \tag{9}$$

have been derived from the fetch relations (2) and (3) through the following space–time conversion relation (see appendix):

$$gF/U_*^2 = 1{\cdot}18 \times 10^{-2}(gt/U_*)^{1{\cdot}555}. \tag{10}$$

As shown schematically in figure 2, the duration-limited wind waves coincide with fetch-limited wind waves at the front of the steady region, and the front can be described by (10). Therefore, on substituting (10) into the fetch relations (2) and (3), we can derive the duration relations (8) and (9). As can be seen from figure 10, the measured duration relations are slightly different but not far from those inferred from the fetch relations.

6. The spectral form of the duration-limited wind waves

Similarity forms for one-dimensional spectra of duration-limited wind waves have been reported by many authors (Pierson & Moskowitz 1964; Colonel 1966; Hidy & Plate 1966; Liu 1971; Mitsuyasu *et al.* 1973; Hasselmann *et al.* 1973). In particular, for the case of laboratory wind waves in a steady state, the one-dimensional spectra normalized in the form

$$\phi(f)f_m/E = \Phi(f/f_m) \tag{11}$$

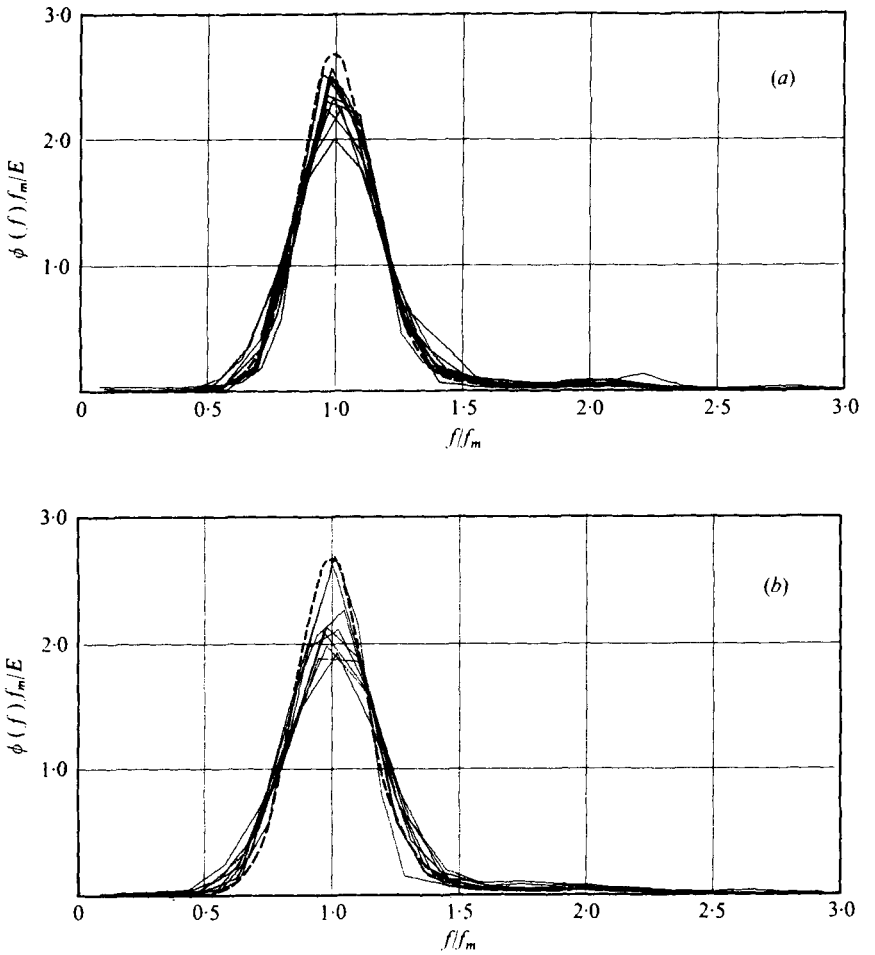

FIGURE 11. Normalized forms of the duration-limited wave spectra compared with the fetch-limited wave spectrum (dashed curve). (*a*) $\bar{U}_* = 0$–$30{\cdot}3$ cm/s, $F = 13$ m. (*b*) $\bar{U}_* = 0$–$30{\cdot}6$ cm/s, $F = 18$ m.

are quite similar with very small deviations over wide ranges of their generating conditions such as the wind speed, the fetch and the width of the wave tank (Mitsuyasu *et al.* 1973, 1975). For the case of ocean waves, however, the normalized spectra (11) show some scatter even under fairly simple generating conditions (Mitsuyasu *et al.* 1975).

Figures 11(*a*) and (*b*) show the normalized spectra of the duration-limited wind waves measured in the present study. In each figure, the spectra of the wind waves at a fixed station and successive duration times are shown in normalized form. The broken line represents a normalized spectrum of steady-state fetch-limited wind waves which corresponds to the previous data of group *A* (Mitsuyasu *et al.* 1973). It can be seen from these figures that the concentration of the spectral energy near the spectral peak frequency is much smaller for the duration-limited wind waves in the initial stage than for the fetch-limited wind waves in the steady state. Moreover, the deviation of the normalized spectra is relatively large for the duration-limited wind waves.

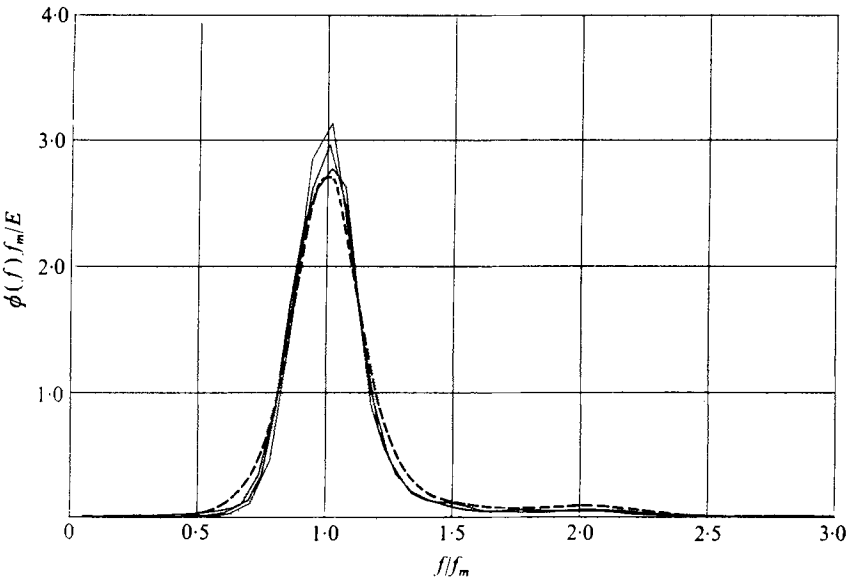

FIGURE 12. Normalized forms of the fetch-limited wave spectra.
$\bar{U}_* = 30{\cdot}6$ cm/s, $F = 8$, 13, 18 m. ----, previous data.

The deviation of the normalized spectra is not necessarily due to the short length of the wave data. Our recent study (Rikiishi & Mitsuyasu 1976) has shown that the energy-containing part of the frequency spectrum determined from short lengths of wave data containing 20–25 waves is very close to that determined from sufficiently long lengths of wave data. Therefore it can be said that the spectral forms of the duration-limited wind waves are not similar but seem to depend on the duration time. This may be one of the reasons why the spectral forms of ocean waves are different from one another even under relatively simple generating conditions, since in many cases ocean waves are duration limited rather than fetch limited owing to their large fetches.

With increasing duration time, however, the normalized spectral energy concentrates gradually towards the spectral peak frequency, and the normalized spectral form finally attains that of fetch-limited wind waves in the steady state. Figure 12 shows the normalized spectra of the wind waves that were measured in this study at fetches $F = 8$, 13 and 18 m for a friction velocity $\bar{U}_* = 30{\cdot}6$ cm/s, which had already attained a steady state. In the figure, the mean spectral form of the previous wave data of group A is shown as a broken curve. It can be seen from figure 12 that the normalized spectra of the fetch-limited wind waves in the different fetches are quite similar to one another, and coincide almost exactly with the previous ones.

Although the spectral data at $F = 3$ m are not shown in figure 12, they are slightly different from the other data shown in the figure. This is perhaps due to the effect of the extremely short fetch. That is, wind waves at very short fetches or very small wind speeds seem to show slightly different properties compared with those at moderate or large fetches and moderate wind speeds. A similar phenomenon was also found in the fetch relations as mentioned briefly in § 5.

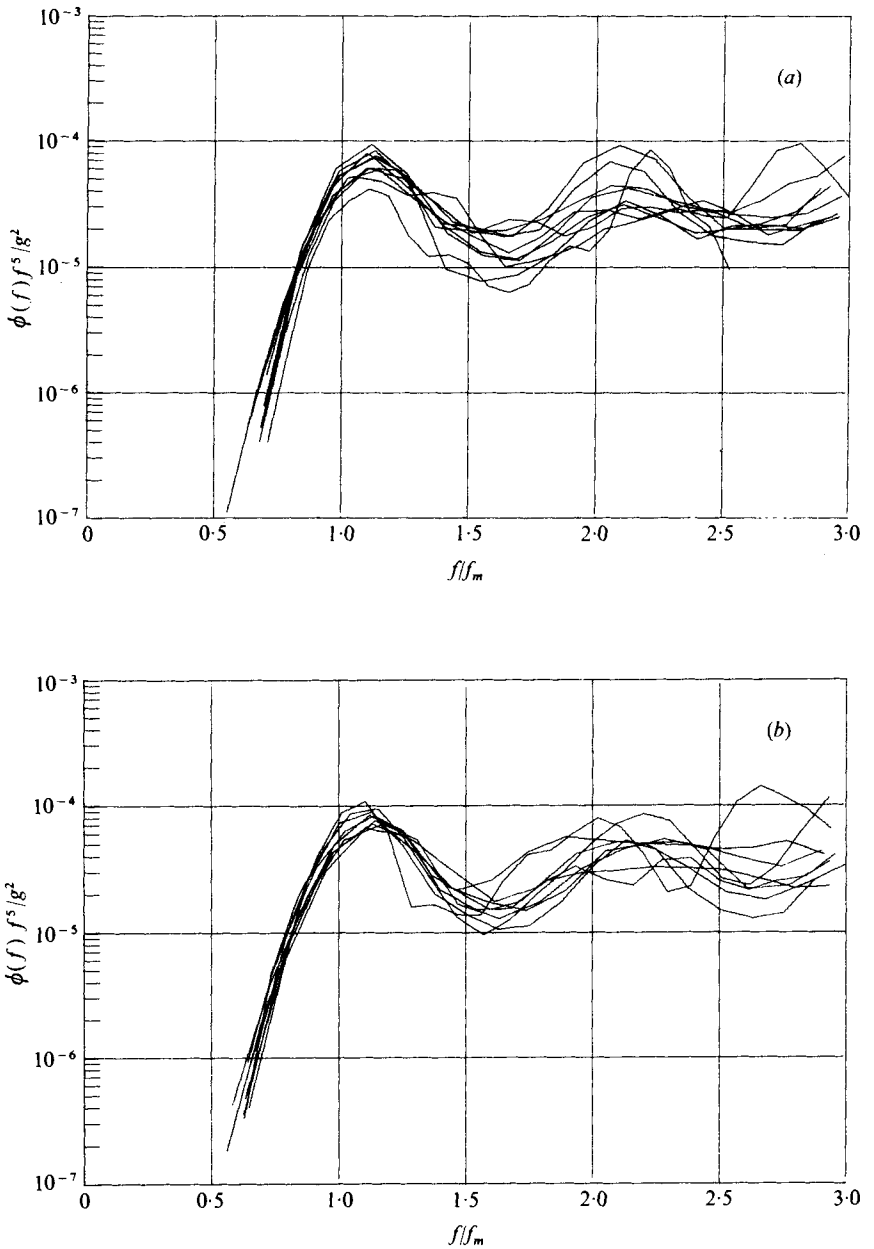

FIGURE 13. Normalized forms of the duration-limited wave spectra. (*a*) $\bar{U}_* = 0$–30·3 cm/s, $F = 13$ m. (*b*) $\bar{U}_* = 0$–30·6 cm/s, $F = 18$ m.

The wave spectrum normalized in the form

$$\phi(f)f^5/g^2 = \psi(f/f_m) \tag{12}$$

is convenient for investigating the high-frequency part of the wave spectrum. This is because in the high-frequency part, where $\phi(f)$ is roughly proportional to f^{-5} (Phillips 1958), the normalized spectrum (12) has an almost constant value, and the fine-

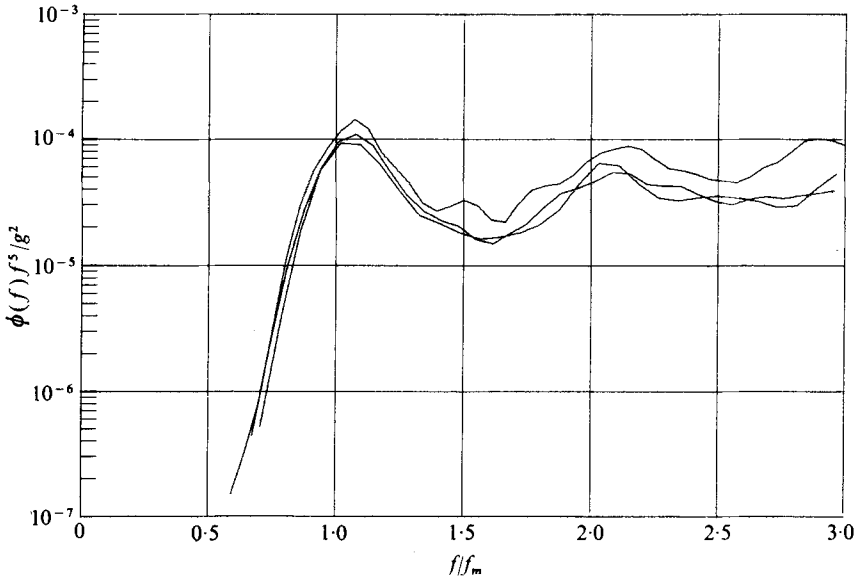

FIGURE 14. Normalized forms of the fetch-limited wave spectra.
$\bar{U}_* = 30{\cdot}6$ cm/s, $F = 8$, 13, 18 m.

structure of the wave spectrum can be seen more clearly in this normalized form. Figures 13 (*a*) and (*b*) show duration-limited wave spectra normalized in the form (12), comprising the same spectral data as are shown in figures 11 (*a*) and (*b*) under the different normalization (11). Figure 14 shows the normalized spectra of the fetch-limited wind waves that are shown in figure 12 under the former normalization.

It can be seen from figures 13 and 14 that secondary and tertiary peaks near the frequencies $2f_m$ and $3f_m$ in the normalized spectra exist for the duration-limited wind waves as well as for the fetch-limited wind waves. These peaks are due to nonlinear effects of the spectral components near the dominant peak of the spectrum (Tick 1959; Mitsuyasu 1969). Therefore the nonlinear effects in the spectrum cannot be negligible even for duration-limited wind waves except for the very early stages of the wave generation.

7. Growth of the spectral components in wind-generated waves

As shown in figure 9, the spectral densities on the low-frequency side of the duration-limited wave spectrum increase with time in a way similar to that observed in the case of a fetch-limited wave spectrum developing with fetch. In order to study the growth rate of the spectral component, the spectral densities on the low-frequency side of the wave spectrum measured at a fixed station were plotted on a logarithmic scale against the duration t on a linear scale. Typical examples are shown in figure 15. It can be seen from this figure that in the stage of rapid growth of the spectral density the relation between $\phi(f,t)$ and t can be approximated by a straight line on a semi-logarithmic plot. That is, the growth of the spectral component is exponential with respect to the time t at that stage. Later, the spectral density saturates and approaches a constant value in an oscillatory manner.

D [$\bar{U}_*$ (cm/s)]	F (m)	f (Hz)	β (s^{-1})	β/f	$\bar{U}_*/C$	f/f_m	$(gF/\bar{U}_*^2)$ $\times 10^{-3}$
15	13	1·953	0·487	0·250	0·379	0·55	1·39
[30·3]		2·344	0·423	0·180	0·455	0·66	1·39
		2·734	0·430	0·157	0·531	0·72	1·39
		3·125	0·379	0·121	0·607	0·77	1·39
15	18	1·563	0·253	0·162	0·307	0·50	1·88
[30·6]		1·953	0·285	0·146	0·383	0·63	1·88
		2·344	0·280	0·119	0·460	0·65	1·88
		2·734	0·306	0·112	0·536	0·73	1·88

TABLE 2. The exponential growth rate (duration-limited wind waves).

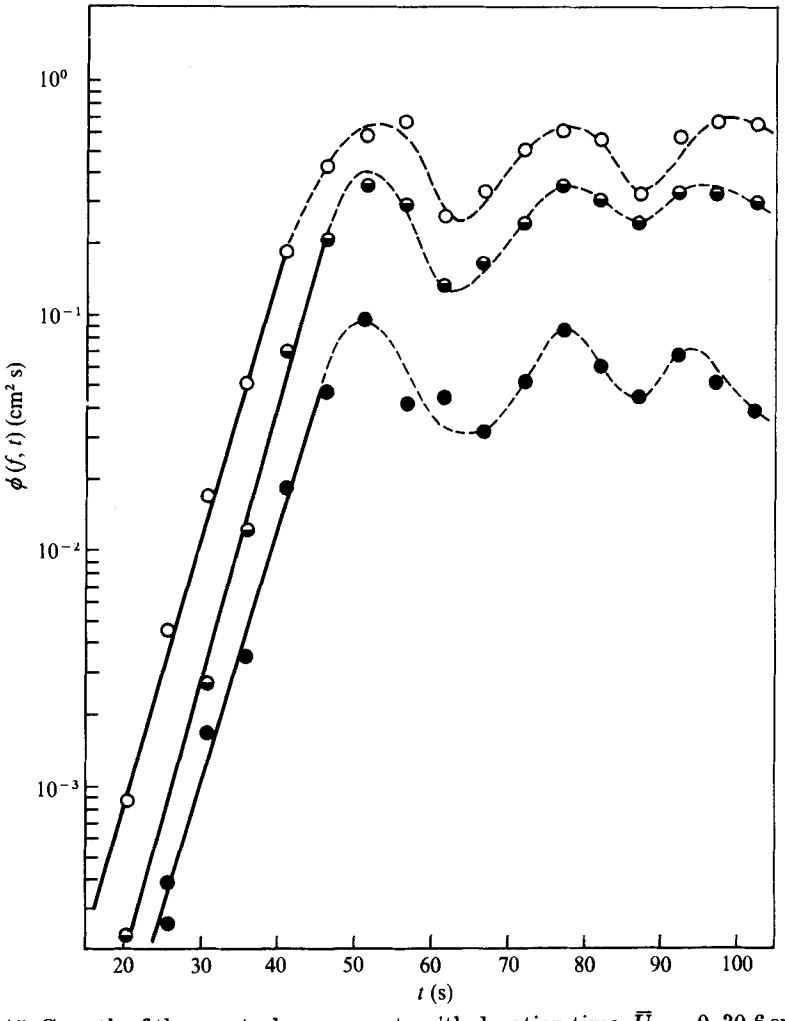

FIGURE 15. Growth of the spectral components with duration time. $\bar{U}_* = 0$–30·6 cm/s, $F = 18$ m. ●, $f = 1{\cdot}563$ Hz; ◒, $f = 1{\cdot}953$ Hz; ○, $f = 2{\cdot}344$ Hz.

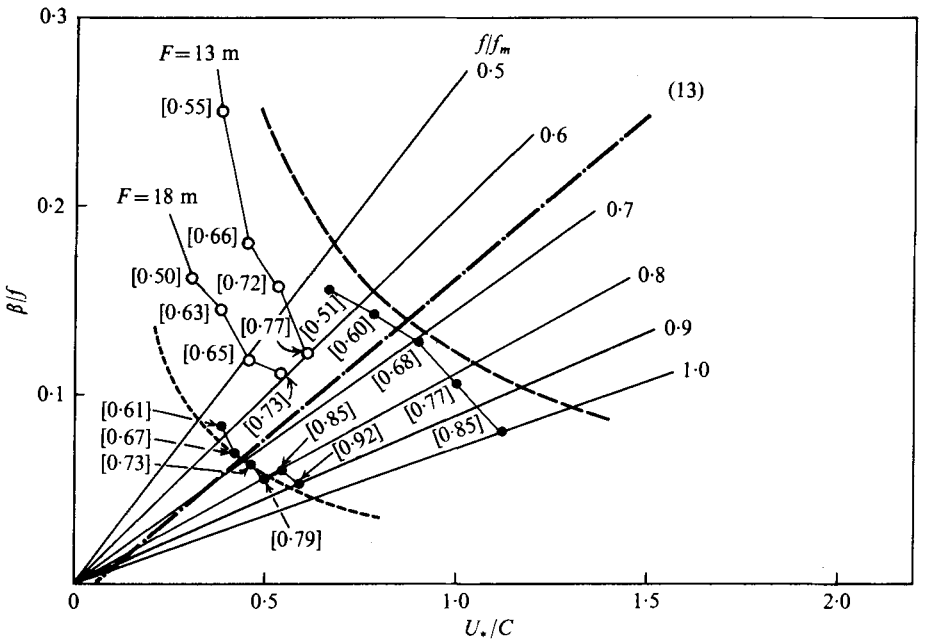

FIGURE 16. Dimensionless exponential growth rate β/f *vs.* dimensionless friction velocity U_*/C of the wind. —○—, growth rate of the duration-limited wave spectrum; —●—, growth rate of the fetch-limited wave spectrum; —·—, equation (13), Synder & Cox (1966); ——, equation (21) for $gF/U_*^2 = 1{\cdot}3 \times 10^2$; – – – –, equation (21) for $gF/U_*^2 = 1{\cdot}1 \times 10^3$; ——, equation (22) for $gF/U_*^2 = 10^3$ and various values of f/f_m. The values in square brackets are the f/f_m values for each data point.

The values of the exponential growth rate β were determined, by the method of least squares, from the gradients of the straight lines. The results are summarized in table 2, where f/f_m is the frequency of the spectral component normalized by the spectral peak frequency f_m. Since the wave spectrum in the present case is changing with time, the spectral peak frequency f_m changes with time and so does f/f_m for a fixed frequency f. The values of f/f_m shown in table 2 correspond to those for the central data on $\phi(f, t)$ which are used for the determination of β. The dimensionless fetch $gF/\overline{U}_*^2$ is shown in the last column.

Figure 16 shows the dimensionless exponential growth rate β/f as a function of the dimensionless friction velocity of the wind U_*/C. For comparison with the experimental result, the contracted form of the empirical relation of Snyder & Cox (1966),

$$\beta/f = 2\pi s\,[22{\cdot}6(U_*/C) - 1], \tag{13}$$

is shown in the figure, where s is the ratio of the densities of air and water. Relation (13) can be obtained from their original relation by assuming $W_1 = 25U_*$ and a directional spectrum of the form $(\frac{8}{3}\pi^{-1})\cos^4\theta$, where W_1 is the mean wind speed at a critical wavelength above the water surface.

In figure 16, each group of data connected with thin lines corresponds to data measured at the same fetch and the same wind speed but for different frequencies. In other words, these data correspond to the dimensionless growth rates of different frequency components in some particular wave spectrum. It can be seen from figure

D [$\bar{U}_*$ (cm/s)]	F (m)	f (Hz)	β (s^{-1})	β/f	$\bar{U}_*/C$	f/f_m	$(gF/\bar{U}_*^2)$ $\times 10^{-2}$
15	13·0	1·953	0·162	0·0827	0·383	0·61	13·6
[30·6]	10·5	2·148	0·148	0·0687	0·422	0·67	11·0
	10·5	2·344	0·148	0·0632	0·460	0·73	11·0
	10·5	2·539	0·140	0·0551	0·498	0·79	11·0
	8·0	2·734	0·164	0·0601	0·537	0·85	8·37
	8·0	2·930	0·155	0·0528	0·575	0·92	8·37
50	10·5	1·172	0·182	0·155	0·672	0·51	1·29
[89·4]	10·5	1·367	0·195	0·142	0·784	0·60	1·29
	10·5	1·563	0·199	0·128	0·896	0·68	1·29
	10·5	1·758	0·186	0·106	1·01	0·77	1·29
	10·5	1·953	0·156	0·080	1·12	0·85	1·29

TABLE 3. The exponential growth rate (fetch-limited wind waves).

16 that in each group of data β/f decreases with increasing U_*/C. However, this does not imply a decrease of β/f with increasing wind speed: because

$$U_*/C = 2\pi U_* f/g \tag{14}$$

and U_* has a constant value for each group, the above result means that β/f decreases with increasing frequency f of the spectral component. This is a natural consequence of the fact that the exponential growth rate β shown in table 2 is roughly constant irrespective of the frequency of the spectral component. Such properties of the dimensionless exponential growth rate found from these experiments are very different from the empirical relation (13).

In order to check these properties of β/f for the case of steady-state fetch-limited wind waves, the growth rates β/f were determined from the measured spectra of steady-state fetch-limited wind waves. In this case, since $\partial\phi/\partial t = 0$, β was determined from spectral data measured at the successive stations (F = 3, 8, 13, 18 m) by using the equation

$$C_g\,\partial\phi(f,x)/\partial x = \beta\phi(f,x). \tag{15}$$

In practice, the value of β/C_g was determined from the mean gradient of log ϕ in a certain range of the fetch, the centre of which is shown in table 3, and then converted to β by multiplying by $C_g(=g/4\pi f)$. In a strict sense, C_g in (15) should be replaced by the directionally averaged group velocity in the x direction:

$$\bar{C}_g = \int_0^{2\pi} C_g \cos\theta F(f,\theta,x)\,d\theta/\phi(f,x), \tag{16}$$

where $F(f, \theta, x)$ is the directional spectrum of the wind waves. However, we used C_g instead of $\bar{C}_g$ because we had no reliable information about the directional spectrum. For spectra with fairly narrow directional distributions, C_g is not much different from $\bar{C}_g$; for example, if we assume a directional spectrum proportional to $\cos^4\theta$, $\bar{C}_g$ becomes $0{\cdot}91C_g$.

The exponential growth rates of the fetch-limited wind waves are summarized in table 3 and their dimensionless values plotted in figure 16 as solid circles. In table 3, f_m is the spectral peak frequency at each fetch shown in the table. When the centre of the fetch F was between two successive stations, f_m was interpolated from its values

at two stations. As can be seen clearly from the figure, for the fetch-limited wind waves β/f shows almost the same trend as for the duration-limited wind waves, though the fetch-limited values are smaller for the same value of U_*/C. Quite similar results have been obtained from the analysis of other recent data on fetch-limited wind waves, though they are not shown in figure 16. Therefore it can be concluded that the dimensionless exponential growth rates β/f measured in our laboratory tank are quite different not only quantitatively but also qualitatively from those given by the empirical relation, and such differences can be seen both for the duration-limited wind waves and for the fetch-limited wind waves. Furthermore, we can confirm our preliminary results that the growth rates of the duration-limited wind waves are larger than those of the fetch-limited wind waves.

8. Discussion

The property of the exponential growth rate shown in figure 16 is one of the most interesting results of the present study. In a sense, the order of magnitude of the exponential growth rate measured in the present experiment is fairly close to that predicted by the empirical relation of Snyder & Cox (1966), particularly for the fetch-limited wind waves. This is a remarkable result, because the empirical relation was originally determined from wave data in the ocean ($U_*/C < 0{\cdot}08$), whereas our results were obtained from those in the laboratory ($0{\cdot}3 < U_*/C < 1{\cdot}8$). Owing to the considerable difference in U_*/C, the generation mechanisms of the wind waves may be different.

However, the exponential growth rate of the present study has another feature, which is quite different from the empirical relation. That is, the dimensionless growth rate β/f decreases with increasing U_*/C ($=2\pi f U_*/g$) in each spectrum.

In order to clarify the general properties of the growth rate, the similarity form of the wave spectrum will be studied, because the growth rate of the spectral component can be determined from the growth pattern of the wave spectrum. In previous studies, one of the present authors determined the similarity form of the spectrum for fetch-limited wind waves using various wave data obtained in a laboratory tank, in a bay and in the open sea (Mitsuyasu 1968, 1973). According to these studies, the spectral form below the spectral peak frequency f_m can be represented by

$$\phi(f) = 5{\cdot}86 \times 10^{-13} g^2 f^{-5} \exp\left[22{\cdot}1 (gF/U_*^2)^{0{\cdot}312} U_* f/g\right] \quad \text{for} \quad f_c < f < f_m, \tag{17}$$

where $f_c (\cong 0{\cdot}3 f_m)$ is the lower limit of the frequency range where the spectral form (17) is applicable. Recently, Ramamonjiarisoa (1973) also confirmed the spectral form (17). First of all, it should be mentioned that in (17) the exponential growth is not linear with respect to the fetch F; the exponential growth rate changes with the fetch. If we define the local exponential growth rate β as

$$\beta = C_g \partial \log \phi / \partial F, \tag{18}$$

β is given from (17) by

$$\beta = 0{\cdot}549 g^{0{\cdot}312} F^{-0{\cdot}688} U_*^{0{\cdot}376}, \tag{19}$$

and its dimensionless form is

$$U_* \beta/g = 0{\cdot}549 (gF/U_*^2)^{-0{\cdot}688}, \tag{20}$$

or

$$\beta/f = 3{\cdot}45 (gF/U_*^2)^{-0{\cdot}688} (U_*/C)^{-1}. \tag{21}$$

According to (19), β is independent of the frequency f and increases with decreasing fetch F or with increasing friction velocity U_* of the wind. These properties can be seen in our present results shown in tables 2 and 3.

The exponential growth rates determined from (21) are also compared in figure 16 with the present experimental results. As can be seen from this figure, the agreement is quite satisfactory for the case of fetch-limited wind waves. The growth rates for the duration-limited wind waves are much larger than those determined from (21), but the qualitative features of the measured growth rate are quite similar to (21). Therefore we can say that the peculiar characteristics of our measured growth rate are universal at least qualitatively, and that the growth rates of the duration-limited wind waves are larger than those of the fetch-limited wind waves. Furthermore, we can use (20) or (21) to determine the exponential growth rate of the fetch-limited wind waves.

However, several questions arise. Why or under what conditions was the empirical formula (13) obtained? Why is the exponential growth rate larger for the duration-limited wind waves than for the fetch-limited wind waves? What kind of physical mechanism is responsible for such peculiar characteristics of the growth rate of wind waves?

To answer the first question, (21) is modified, using the fetch relation (5), to

$$\frac{\beta}{f} = 0{\cdot}087 \left(\frac{gF}{U_*^2}\right)^{-0{\cdot}028} \left(\frac{f}{f_m}\right)^{-2} \frac{U_*}{C}. \tag{22}$$

Note that this form for β/f is almost independent of the dimensionless fetch gF/U_*^2, if the value of f/f_m is fixed. Then, if we put

$$gF/U_*^2 = 10^3, \quad f/f_m = 0{\cdot}7,$$

(22) reduces to

$$\beta/f = 0{\cdot}147 U_*/C. \tag{23}$$

This is almost the same form as the empirical relation of Snyder & Cox (1966). Relation (22) for typical values of f/f_m is shown in figure 16 for the case $gF/U_*^2 = 10^3$. It can be seen that the measured values of β/f are very close to (22) for the case of fetch-limited wind waves. Therefore it can be said that an empirical relation of the form of Snyder & Cox's (1966) can be obtained when we measure the growth rate of the spectral component for an assigned relative frequency f/f_m. In fact, in the observations of Snyder & Cox, the effective fetches where the growth rate of the spectral component was determined were roughly proportional to W_1^{-1} and therefore U_*^{-1} (Snyder 1965). From (5), this is about what is required to make f_m and therefore f/f_m constant.

In order to answer the other two questions we consider the one-dimensional transport equation

$$\partial\phi(f,x,t)/\partial t + \bar{C}_g\, \partial\phi(f,x,t)/\partial x = S, \tag{24}$$

which can be obtained by integrating the two-dimensional transport equation (Hasselmann 1968) with respect to the propagation direction θ. Here S is the net source function, which may be divided generally into three terms

$$S = S_{in} + S_{nl} + S_{ds} \tag{25}$$

representing, respectively, the energy input S_{in} from the wind, the nonlinear energy transfer S_{nl} due to conservative wave–wave interactions and a dissipation term S_{ds}.

The preliminary analysis of our measured spectral data has shown that, in the transition ranges of our duration-limited wind waves, the convective term on the left-hand side of (24) is much smaller than the first local term. Hence (24) can be approximated, in our case, by

$$\partial\phi(f,x,t)/\partial t = S_{in}+S_{nl}+S_{ds}. \tag{26}$$

Nonlinear wave–wave interactions may be responsible for the physical mechanism of wave generation which produces the peculiar properties of the exponential growth rate. From most of the mechanisms which transfer momentum from the wind to the waves, the following expression for the exponential growth rate can be obtained:

$$\beta/f \propto s(U_*/C)^n, \tag{27}$$

where $n = 1$ or 2. This form is quite different from our measured results shown in figure 16. Furthermore, according to recent studies of the growth of the wave spectrum, the rapid growth of the spectral densities in a frequency range below the spectral peak frequency f_m is largely attributed to the nonlinear wave–wave interactions (Sell & Hasselmann 1972), and the energy input from the wind to the wave seems to be dominant only in the relatively narrow central region of the wave spectrum (Hasselmann *et al.* 1973). Consequently, the value of $\partial\phi/\partial t$ on the forward face of our measured spectrum may not be attributed to the energy input S_{in} through direct wind–wave interaction, but may correspond mostly to the nonlinear energy transfer S_{nl} and only partly to the energy input S_{in} and the energy dissipation S_{ds}. The expression (21) for the exponential growth rate is considered to reflect such dynamical process of wind-wave generation.

The energy dissipation S_{ds} in our case can be attributed to wave breaking and to viscous dissipation in the boundary layer near the side walls of the tank and in the surface shear zone. However, the viscous dissipation was found to be negligible on the low-frequency side of our measured spectrum, where the growth rate was examined. Thus most of the energy dissipation in that frequency range is due to wave breaking, though its quantitative evaluation is very difficult. The considerable difference in the values of the exponential growth rates for the fetch-limited wind waves and the duration-limited wind waves may be attributed partly to the difference in the magnitude of energy dissipation due to the wave breaking in these two wave systems. Some of the difference in the growth rates may be attributed partly to the effect of the drift current. If we consider a drift current to co-exist with the wind waves, the convection velocity of the spectral energy is larger than $C_g(=g/4\pi f)$, and thus determination of β from (15) without taking the effect of the drift current into account underestimates the value of β.

The experimental study conducted recently by Larson & Wright (1975) is quite similar to our present study except that they measured very short waves (wavelength = 0·7–7 cm) by using microwave backscatter. However, their measured growth rates of duration-limited wind waves show properties different from ours; the temporal growth rate is approximately proportional to $U_*^{\frac{3}{2}}$ whereas our results give a value proportional to $U_*^{0\cdot376}$ as shown in (19). The difference between their result and ours may be attributed to the difference between the frequency ranges measured. The frequencies of the spectral components measured by Larson & Wright (1975) are

4·9–38 Hz, which are much higher than the frequencies 1·1–3·1 Hz of our measured spectral components for which the growth rates were computed. Such high-frequency waves as those measured by Larson & Wright (1975) develop so rapidly that nonlinear wave–wave interactions and consequently their effect on β might be much smaller than those in our experiment.

9. Summary and conclusions

The temporal growths of the wave energy E and the spectral peak frequency f_m for the duration-limited wind waves are slightly different from those inferred from the spatial growths of these quantities for the steady-state fetch-limited wind waves. For practical purposes, however, we may use the duration relations inferred from the fetch relations by using the space–time conversion relation (10), because the differences between the measured and the inferred spectra are relatively small.

The normalized spectra $\phi(f)f_m/E$ for the duration-limited wind waves are slightly different from one another depending on the duration time, whereas the normalized spectra are quite similar for the steady-state fetch-limited wind waves. The concentration of the normalized spectral energy near the spectral peak frequency is smaller for the duration-limited wind waves in the initial stage than for the steady-state fetch-limited wind waves. Typical nonlinear features in the wave spectrum, secondary and tertiary peaks near the frequencies $2f_m$ and $3f_m$, are found for the duration-limited waves as well as for fetch-limited waves.

The exponential growth rate β of the duration-limited wind waves is much larger than that of the fetch-limited wind waves. Furthermore, both for the duration-limited wind waves and for the fetch-limited wind waves the exponential growth rate shows some peculiar characteristics which cannot be expected from the empirical formula of Snyder & Cox (1966): a dimensionless growth rate β/f which depends not only on the dimensionless wind velocity U_*/C but also on the dimensionless fetch gF/U_*^2. For a fixed value of gF/U_*^2, β/f decreases with increasing U_*/C.

A general relation (21) among β/f, U_*/C and gF/U_*^2 can be derived from a similarity form of the wave spectrum (17) which was obtained in a previous study (Mitsuyasu 1968, 1973). We can use (20) or (21) as the new empirical formula for the growth rate β/f. The present experimental values agree well with (21) for the case of fetch-limited wind waves. For the case of duration-limited wind waves, however, β/f is larger than the values given by (21), though the qualitative features are very similar.

The relation (21) can be transformed into another equivalent relation (22), in which β/f depends mainly on U_*/C and f/f_m and very weakly on gF/U_*^2. If the value of f/f_m is fixed approximately at 0·7 in (22), we can get a relation which is quite similar to the empirical relation of Snyder & Cox (1966).

We are grateful to Professor O. M. Phillips of the Johns Hopkins University for his valuable comments on the manuscript and to reviewers for helpful comments and suggestions. We are also indebted to Dr S. Mizuno and Mr A. Masuda of Kyushu University for useful discussions of the problem. The laboratory experiment was conducted in 1969 by one of the authors with the assistance of Mr R. Nakayama and Mr T. Komori, former research associate of Kyushu University. Their invaluable help is greatly appreciated. The authors are also indebted to Mr K. Eto for his

assistance in the experiment and for drawing the figures, and to Miss N. Uraguchi for typing the manuscript.

Appendix

The time necessary for a wave group to travel from the upwind boundary to a fetch F is given by

$$t = \int_0^F (C_g)^{-1} dF, \tag{A 1}$$

where C_g is a group velocity of the wave system. Equation (A 1) defines the minimum duration $t_{\min}$. Now we assume the relation

$$C_g = g\tilde{T}/4\pi, \tag{A 2}$$

where $\tilde{T}$ is the period of the dominant wave corresponding to the wave system. The dominant wave period $\tilde{T}$ can be related to the spectral peak frequency f_m in the following way.

Let us consider the spectral form

$$\phi(f) = k_1 f^{-m} \exp[-k_2 f^{-n}]. \tag{A 3}$$

The wave period $\tilde{T}$, defined as the zero-up-crossing period, is given by

$$\tilde{T} = \left[\int_0^\infty \phi(f) f^2 df \Big/ \int_0^\infty \phi(f)\, df\right]^{-\frac{1}{2}}. \tag{A 4}$$

After substitution of (A 3), (A 4) reduces to

$$\tilde{T} = k_2^{-1/n} \left[\frac{m-3}{m-1}\right]^{-\frac{1}{2}}. \tag{A 5}$$

On the other hand, the spectral peak frequency f_m of the spectrum (A 3) is given by

$$f_m = (nk_2/m)^{1/n}. \tag{A 6}$$

So, from (A 5) and (A 6),

$$\tilde{T} = \frac{1}{f_m}\left(\frac{n}{m}\right)^{1/n}\left(\frac{m-3}{m-1}\right)^{-\frac{1}{2}} \quad \left(= \frac{\gamma}{f_m}\right). \tag{A 7}$$

Furthermore, if the spectral form is assumed to be of Pierson–Moskowitz type ($m = 5$, $n = 4$), (A 7) reduces to

$$\tilde{T} = 1{\cdot}34 f_m^{-1}, \tag{A 8}$$

and (A 2) becomes

$$C_g = 1{\cdot}34 g/4\pi f_m. \tag{A 9}$$

On substituting (A 9) and the fetch relation (3), i.e.

$$U_* f_m/g = 1{\cdot}19(gF/U_*^2)^{-0{\cdot}357}, \tag{A 10}$$

into (A 1) and carrying out the integration we get the space–time conversion relation

$$gF/U_*^2 = 1{\cdot}18 \times 10^{-2}(gt/U_*)^{1{\cdot}555}. \tag{A11}$$

This relation describes the front of the steady state, where duration-limited wind waves coincide with fetch-limited wind waves.

REFERENCES

BARNETT, T. P. 1968 On the generation, dissipation, and prediction of ocean wind waves. *J. Geophys. Res.* **73**, 513–529.

COLONEL, J. M. 1966 Laboratory simulation of sea waves. *Dept. Civil Engng, Stanford Univ. Tech. Rep.* no. 65.

DELEONIBUS, P. S. & SIMPSON, L. S. 1972 Case study of duration-limited wave spectra observed at an open ocean tower. *J. Geophys. Res.* **77**, 4555–4569.

HASSELMANN, K. 1968 Weak interaction theory of ocean surface waves. In *Basic Developments in Fluid Mechanics*, § 5.2. Academic Press.

HASSELMANN, K. *et al.* 1973 Measurements of wind-wave growth and swell decay during the Joint North Sea Wave Project (JONSWAP). *Dtsch. Hydrogr. Z.* **12**, 1-95.

HIDY, G. M. & PLATE, E. J. 1966 Wind action on water standing in a laboratory channel. *J. Fluid Mech.* **26**, 651–687.

INOUE, T. 1966 On the growth of the spectrum of a wind-generated sea according to a modified Miles–Phillips mechanism. *Dept Met. Ocean., New York Univ. Rep.* TR 66-6.

IWATA, N. & TANAKA, T. 1970 Spectral development of wind waves. *Nat. Res. Center Disaster Prevention Japan Rep.* no. 4, pp. 1–21 (in Japanese).

LARSON, T. R. & WRIGHT, J. W. 1975 Wind-generated gravity–capillary waves: laboratory measurements of temporal growth rates using microwave backscatter. *J. Fluid Mech.* **70**, 417–436.

LIU, P. C. 1971 Normalized and equilibrium spectra of wind waves in Lake Michigan. *J. Phys. Ocean.* **1**, 249–257.

MITSUYASU, H. 1968 On the growth of the spectrum of wind-generated waves (I). *Rep. Res. Inst. Appl. Mech., Kyushu Univ.* **16**, 459–482.

MITSUYASU, H. 1969 On the growth of the spectrum of wind-generated waves (II). *Rep. Res. Inst. Appl. Mech., Kyushu Univ.* **17**, 235–248.

MITSUYASU, H. 1973 The one-dimensional wave spectra at limited fetch. *Rep. Res. Inst. Appl. Mech., Kyushu Univ.* **20**, 37–53.

MITSUYASU, H. & HONDA, T. 1974 The high frequency spectrum of wind-generated waves. *J. Ocean. Soc. Japan* **30**, 185–198.

MITSUYASU, H. & RIKIISHI, K. 1972 On the growth of duration-limited wave spectra. *Ann. Conf. Ocean. Soc. Japan.*

MITSUYASU, H. *et al.* 1973 Laboratory simulation of ocean waves. *Bull. Res. Inst. Appl. Mech., Kyushu Univ.* no. 39, pp. 183–210 (in Japanese).

MITSUYASU, H. *et al.* 1975 Observations of the directional spectrum of ocean waves using a cloverleaf buoy. *J. Phys. Ocean.* **5**, 750–760.

PHILLIPS, O. M. 1958 The equilibrium range in the spectrum of wind-generated ocean waves. *J. Fluid Mech.* **4**, 426–434.

PIERSON, W. J. & MOSKOWITZ, L. 1964 A proposed spectral form for fully developed seas based on the similarity theory of S. A. Kitaigorodskii. *J. Geophys. Res.* **69**, 5181–5190.

PRIESTLEY, M. B. 1965 Evolutionary spectra and non-stationary processes. *J. Roy. Statist. Soc.* B **27**, 204–237.

PRIESTLEY, M. B. 1966 Design relation for non-stationary processes. *J. Roy. Statist. Soc.* B **28**, 228–240.

PRIESTLEY, M. B. 1967 Power spectral analysis of non-stationary random process. *J. Sound Vib.* **6**, 86–97.

RAMAMONJIARISOA, A. 1973 Sur l'évolution des spectres d'énergie des vagues de vent à fetchs courts. *Mém. Soc. Roy. Sci. Liège* **6**, 47–66.

RIKIISHI, K. & MITSUYASU, H. 1976 Notes on the effects of data length and sampling interval upon the spectral estimates for wind waves. *Rep. Res. Inst. Appl. Mech., Kyushu Univ.* **23**, 131–147.

SELL, W. & HASSELMANN, K. 1972 Computation of nonlinear energy transfer for JONSWAP and empirical wind wave spectra. *Rep. Inst. Geophys., Univ. Hamburg.*

SNYDER, R. L. 1965 The wind generation of ocean waves. Ph.D. dissertation, University of California, San Diego.

SNYDER, R. L. & COX, C. S. 1966 A field study of the wind generation of ocean waves. *J. Mar. Res.* **24**, 141–178.

TAIRA, K. 1972 A field study of the development of wind-waves. Part 1. The experiment. *J. Ocean. Soc. Japan* **28**, 187–202.

TICK, L. J. 1959 A non-linear random model of gravity waves I. *J. Math. Mech.* **8**, 643–651.